Final Draft
of the original manuscript:

Neffe, A.T.; Loebus, A.; Zaupa, A.; Stoetzel, C.; Mueller, F.A.; Lendlein, A.:
Gelatin Functionalization with Tyrosine Derived Moieties for Increasing the Interaction with Hydroxyapatite Fillers
In: Acta Biomaterialia (2010) Elsevier

DOI: 10.1016/j.actbio.2010.11.025

Gelatin Functionalization with Tyrosine Derived Moieties for Increasing the Interaction with Hydroxyapatite Fillers

Axel T. Neffe,[1,2,*] Axel Loebus,[1,3] Alessandro Zaupa,[1,2] Christian Stoetzel,[3] Frank A. Mueller,[3] Andreas Lendlein[1,2]

1: Center for Biomaterial Development and Berlin-Brandenburg Center for Regenerative Therapies, GKSS Research Centre Geesthacht GmbH, Kantstrasse 55, 14513 Teltow

2: Institute of Chemistry, University of Potsdam, 14476 Potsdam-Golm

3: Institute of Materials Science and Technology (IMT), Friedrich-Schiller-University of Jena, Löbdergraben 32, D-07743 JENA

*Corresponding Author: Axel T. Neffe, Center for Biomaterial Development and Berlin-Brandenburg Center for Regenerative Therapies, GKSS Research Centre Geesthacht GmbH, Kantstrasse 55, 14513 Teltow, Germany, Email-address: axel.neffe@gkss.de, Fax: +49-3328-352452, Tel: +49-3328-325325

Abstract:

Combining gelatins functionalized with the tyrosine-derived groups desaminotyrosine or desaminotyrosyl tyrosine with hydroxyapatite (HAp) led to the formation of composite materials with much lower swelling ratio than of the pure matrices or pure gelatin. Shifts of IR bands related to the free carboxyl groups could be observed in the presence of HAp, which suggested a direct interaction of matrix and filler that formed additional physical crosslinks in the material. In tensile tests and rheological measurements, the composites equilibrated in water had increased Young's moduli (from 200 kPa up to 2 MPa) and tensile strength (from 57 kPa up to 1.1 MPa) compared to the matrix polymers without affecting the elongation at break. Furthermore, an increased thermal stability from 40 °C to 85 °C of the networks could be demonstrated. The differences of the behaviour of the functionalized gelatins to pure gelatin as matrix suggested an additional stabilizing bond between the incorporated aromatic

groups to the hydroxyapatite as supported by the IR results. The composites can potentially be applied as bone fillers.

Keywords: Gelatin, Hydroxyapatite, Composite, Hydrogel, Biomaterial

1. Introduction

Nature uses composites to generate materials that exhibit high mechanical stability combined with elasticity. In the composites, inorganic micro- or nano-sized fillers are distributed in a (bio)polymer matrix which binds the filler together and protects the filler from damage by stress distribution [1]. The increase of material properties of the composites depends amongst others on i) the original properties of the matrix, ii) the filler content, iii) the filler size and form, and iv) the interaction between filler and matrix [2]. In technical applications, fillers with high aspect ratios such as layered silicates or carbon nanotubes are often used as they already show strong effects even when only small weight percentages of filler is incorporated [3,4]. However, particulate fillers with small aspect ratios are important for mimicking biological materials. Biomineral fillers important in biological composite materials include calcium phosphates, calcium carbonates, and silica. In vertebrates, calcium phosphates represent the most important class. Hydroxyapatite (HAp), in form of carbonate containing calcium phosphates, is present in bone, teeth, and tendons and has also been applied as an implanted biomaterial [5,6].

It has been shown that the biocompatibility of materials in contact with osteoblasts in cell culture and with bone in the living system can be increased by incorporating calcium phosphates such as tricalciumphosphate or HAp [7-11]. One observation in this respect is the better contact between bone and implant [12], as these interactions at the interface are important in bone and implant remodelling processes [13]. The natural matrix in bone is mainly collagen I [14], which therefore has been investigated extensively. Composites of HAp dispersed in collagen or other matrices can be prepared by incorporating pre-fabricated

calcium phosphate or (carbonated) HAp particles into the respective matrix [15,16]. In addition to films, composite scaffolds have also been prepared [17,18].

The interaction between matrix and filler generally has a strong effect on the maximum tensile strength of the composite. On the one hand, particle size and surface area play an important role for the interaction between matrix and filler, and consequently nanoparticles often have a stronger effect on material properties than microparticles [19,20]. On the other hand, specific chemical functionalization of the filler may increase the interaction between filler and matrix [21,22]. Modelling studies have shown that in biological composites matrices seem to specifically interact with their fillers [23,24]. In the design of a biomaterial, the use of a biopolymer is beneficial in terms of providing as well sites of adhesion for cells (e.g. DGEA and GFOGER in collagen or gelatin) as sites susceptible to cleavage by proteases, which otherwise would have to be incorporated into a material to allow replacement of the material over time by functional neo-tissue [25,26]. However, the tailoring of material properties is challenging in view of the inherent self-organization of biopolymers in physiological environments and variability between production batches [27].

Here we wanted to explore whether it is possible to alter composite material macroscopic properties by changing the interaction of filler and matrix by systematically varying the polymer properties, thereby developing a polymer composite system, i.e. a closely related family of materials in which already small changes in the structure have remarkable effects on macroscopic properties [28-30]. Therefore, especially the water uptake and swelling, mechanical properties, and the thermal transitions of the composites compared to the pure matrix were of interest. Because of the intended application, all mechanical properties were determined under conditions relevant to potential biomedical applications, i.e. under equilibrium swelling.

The choice of materials was guided by nature, so that a biopolymer/filler combination should be used that on the one hand is close to a biological system and on the other hand allows the necessary chemical functionalization. The macroscopic properties of the composites should be ruled by both components, while the local elasticities should predominantly be

ruled by the matrices. In physiological environment, the Young's modulus (*E*) of the matrix should be in the kPa range, corresponding to the demands for cell adhesion and differentiation [31,32]. By using a protein as matrix, functionalization of free amino groups with aromatic compounds should give compounds in which a increased number of groups is present which potentially can interact with ions on the surface of the filler [33,34]. The introduction of aromatic moieties would also likely lead to a lower water uptake of the matrix due to the increased hydrophobicity of the matrix. Simultaneously, the lower water uptake is likely to increase the overall mechanical properties.

For this purpose, gelatin functionalized with increasing numbers of aromatic groups was chosen as the matrix. Gelatin is derived from collagen, which is the main protein component of the extracellular matrix of bone and plays a key role in bone structure, formation, and healing. Gelatin implants have low immunogenicity and FDA approval as clotting agent [35]. Gelatin-based materials were shown to be tailorable in mechanical properties and swelling by chemical or physical crosslinking when inhibiting the formation of triple helices [36-39]. Potential applications of gelatin-based composites include bone fillers and adhesives, which have bulk Young's moduli in the MPa range [40-42].

In the following, the formation of composite films from pure gelatin, desaminotyrosine (DAT) functionalized gelatin (Gel-DAT) (bearing one aromatic ring per free amino group of gelatin), and desaminotyrosyl tyrosine (DATT) functionalized gelatin (Gel-DATT) (bearing two aromatic rings per free amino group of gelatin) with two types of hydroxyapatite in two different weight ratios are described. The material properties thereby should on the one hand be ruled by the physical crosslinking of the matrix by π–π interactions of the aromatic groups and, potentially, formation of triple helical regions, and furthermore by the matrix-HAp interactions. The films were characterized by IR spectroscopy, SEM/TEM, water uptake and degree of swelling, tensile tests, and rheology to describe the molecular structure of the composites and the effect on the macroscopic properties.

2. Materials and methods

2.1 Materials: Gelatin type A and β-mercaptoethanol were purchased from Fluka (Germany). Desaminotyrosine (DAT), *N*-hydroxysuccinimide (NHS), 1-ethyl-3-(3-dimethyl-aminopropyl) carbodiimide (EDC), and *N*,*N*-Diisopropylethylamine (DIPEA) were purchased from Sigma Aldrich (Germany). Dimethyl Sulfoxide (DMSO) was purchased from Merck (Germany). All reagents and solvents were of analytical grade and used without further purification. DATT, Gel-DAT and Gel-DATT were synthesized as previously described [36].

Carbonated hydroxyapatite (HAp) was synthesized with a wet precipitation method. Synthesis temperatures were set to 22 °C and 100 °C, respectively, while synthesis time was kept constant at 48h. Calcium nitrate tetrahydrate (Carl Roth GmbH & Co. KG, Karlsruhe, Germany) and diammonium hydrogen phosphate (Carl Roth GmbH & Co. KG, Karlsruhe, Germany) were the starting materials. 32 % NH_3 in H_2O solution (Carl Roth GmbH & Co. KG, Karlsruhe, Germany) was used to adjust the pH value to 10. A constant temperature and vigorous magnetic stirring were maintained during the reaction. Following 48 h, the suspension was quickly filtered and washed with sufficient distilled lukewarm water until all ammonia was removed. The resulting cake was dried at 75 °C for at least 24 h and grinded to a homogeneous powder using a ball mill grinding jar. The obtained powders are designated as Type1 (synthesis temperature 22 °C) and Type2 (synthesis temperature 100 °C).

2.2 *Composite hydrogels* were prepared in a mixing process of HAp Type1 or HAp Type2 as inorganic filler and gelatin, Gel-DAT or Gel-DATT as matrix at a weight ratio 1:4 and 1:1. In order to gain homogeneous composite hydrogels, a solution of 20 wt.-% and 50 wt.-% of HAp-powder in respect to applied quantity of gelatin, Gel-DAT or Gel-DATT was dispersed in distilled water under constant magnetic stirring and ultrasonic excitation (25 W, continuous mode; Bandelin Sonopuls HA2070) in order to de-agglomerate the HAp particles, and subsequently combined to a 3 wt.-% aqueous solution of G0, GEL-DAT or GEL-DATT prepared at 70 °C. The obtained mixtures were promptly cast into Petri dishes and allowed to dry at ambient conditions.

2.3 *Thermo-gravimetric Analyses* (TGA) were carried out to quantify the inorganic content within the composites. Measurements were conducted on a thermo microbalance (Netsch GmbH, TG 209C) under Nitrogen atmosphere within a temperature range of 25°C – 850°C at a heating rate of 10 $K \cdot min^{-1}$.

2.4 *Transmission-Electron-Microscopy and Scanning-Electron-Microscope* (Zeiss, Supra 40VP Gemini) were applied to visualize HAp-particle-size and cross-sections of composite hydrogels respectively. TEM samples were prepared by depositing the powder of interest on platinum-nets and applying an acceleration voltage of 80 kV. SEM samples were carbon coated and an acceleration voltage of 10 kV was applied yielding EDX spectra at a penetration depth of around 2 µm. These measurements were conducted towards identifying the Ca/P ratio of HAp Type1 and HAp Type2 incorporated in the composites.

2.5 *Elemental Composition Analysis* (Flash EA 1112 CHNS/O Automatic Elemental Analyser) was carried out in order to determine the Ca/P ratio and to quantify the carbonate contents of pure HAp. The deviation was given as 2 % in the measured range.

2.6 *Specific surface area* (SSA). The BET (Gemini 2370 V4.01) method was conducted to determine the specific surface area of HAp powders. Measurements were conducted over a period of 2 h. Powders were dried at 200 ºC prior to the measurements.

2.7 *Wide-Angle X-ray Scattering* (WAXS) was carried out on a Bruker, AXS D8 Discover, and was employed in order to identify phases present in the investigated material. The crystal-size (X_s), the crystallinity (X_c) and their deviation were estimate the values for the HAp powders, using the following equations:

$$X_s = \frac{0.9 \cdot \lambda}{FWHM \cdot \cos\theta} \qquad \textit{eq. 1}$$

$$X_c = 1 - \left(\frac{V_{112/300}}{I_{300}} \right) \qquad \textit{eq. 2}$$

where λ is the wavelength of the X-rays and *FWHM* is the full width at half maximum of the diffraction peak at the Bragg angle θ, $V_{112/300}$ denotes to the intensity of the valley in the X-ray

spectra between the peaks referring to planes (112) and (300) while I_{300} is the intensity of the peak referred to (300). The X-ray generator was operated at a voltage of 40 kV and a current of 40 mA, producing Cu Kα-radiation with a wavelength λ = 0.154 nm. WAXS images were collected from composite films (thickness of about 0.3 mm, exposure times: 8 minutes) in transmission geometry with a collimator-opening of 0.8 mm at a sample-to-detector distance of 15 cm. Integration of the two-dimensional scattering data gave the intensity as a function of the scattering angle 2θ. A scanning speed of 100 s·degree^{-1} was applied for investigation on HAp powders.

2.8 *Tensile-tests* were conducted on five replicas in order to evaluate mechanical performance. Bone-shaped (20 mm in length and 2 mm in width) samples were punched out of swollen hydrogels, which were allowed to swell at least 12 h prior to measurements. Tests were performed at room temperature at a strain velocity of 1 mm·min^{-1}, due to applied stress (max 1.25 N) during the measurement. Data recording started at a force threshold of 0.01 N. The instrument employed was a universal tension testing machine (Zwick, Z 2.5) with a load cell of 50 N. In order to obtain reliable experimental data, every measurement was repeated five times with different specimens prepared as required in ISO 527-2. The E modulus was calculated deploying the first five percent of strain, while the σ_{max} was determined from the stress-strain curve recorded at ε_b.

2.9 *FTIR measurements* were conducted (Bruker-Optics, α-Alpha-P and Shimadzu, FtIR-8400S) in order to qualitatively examine the changes of some functional groups and identify existing interactions within the composite materials. Measurements performed ranged from 400 cm^{-1} - 4000 cm^{-1} for investigations on pure HAp and 600 cm^{-1} - 4000 cm^{-1} for composite materials. The samples were dried under vacuum for 48 h to remove residual moisture prior to measurement.

2.10 *Degree of Swelling.* Vacuum dried samples were balanced before immersing them into distilled water. Samples were kept there at 22 °C and 37 °C temperature-controlled water bath respectively and removed after 24 h in order to determine the net weight after

gently wiping with a filter-paper to remove residual bulk water. Each set of materials contained five replicas. To quantify water-uptake and swelling, equations 3 and 4 were used.

Water-uptake $$H = \left[\frac{\left(m_{sw} - m_{dry}\right)}{m_{dry}} \right] \cdot 100$$ *eq. 3*

Degree of Swelling $$Q = 1 + \rho_{comp} \left(\frac{m_{sw}}{m_d \rho_{H_2O}} - \frac{1}{\rho_{H_2O}} \right)$$ *eq. 4*

Where m_{sw} refers to net weight of the respective hydrogel in the swollen state, m_{dry} is attributed to vacuum dried weight, ρ_{comp} states the density of the explored composites determined via pycnometry, and ρ_{H2O} is the density of distilled water assumed to be 1.00 $g \cdot cm^{-3}$ (difference between RT and 37 ºC ca. 0.004 $g \cdot cm^{-3}$).

2.11 *Rheological measurements* were performed with disc-disc rheoviscosimeter (Rheotec, Haake MARS Thermo Fischer, RheoWin Software) using a Peltier-element of 20 mm diameter. All the dynamic measurements were performed in the linear viscosity region applying a constant normal force of 1 Pa. All samples were previously swollen in water at equilibrium and a solvent trap was used to prevent evaporation of solvent during measurements. The temperature dependence of the storage modulus was determined by oscillatory shear stress with temperature scan ranging from 15 to 70 °C with a heating rate of 1.8 $K \cdot min^{-1}$ at a constant frequency (1 Hz) and constant stress (1 Pa). The gel dissociation temperature T_{gel} was determined as crossover point of G' and G" temperature functions. When no crossover point was found, T_{Gel} was taken to be the temperature at which the elastic modulus has the maximum slope. In order to identify the crossover point of the hydrogels, it was necessary to determine the appropriate frequency and vertical force on the sample (force controlled measurement). The mechanical spectrum was recorded in order to determine the appropriate frequency ranging from 0.1 up to 10 Hz. A suitable range is found when storage modulus (G') (indicating the elastic property of the network) and the loss modulus (G") (indicating viscous properties of the fluid) are yielding a constant plateau. Subsequently a suitable mechanical stress value was ascertained within a range of 0.01 to

20 Pa, where the same effect could be observed. It was found that 1 Hz as applied frequency and 1 Pa as applied shear stress were appropriate parameters for all measured samples.

3. Results

3.1 Hydroxapatite particles and composite formation

The synthesis of HAp particles was performed at r.t. or +100 °C and denoted as Type 1 and Type 2, respectively. HAp Type 1 had a lower crystallinity and crystal size but higher specific surface area, higher Ca/P ratio, and higher carbonate content than HAp Type 2. The two HAp types however had the same aspect ratio of about 2.5. Using the two types of HAp particles, composites with fillers with different properties could be compared. A summary of the HAp particle properties is given in Table 1.

(HERE TABLE 1)

The particles (HAp Type 1 or Type 2) were mixed (20 or 50 wt.-%) with pure gelatin, Gel-DAT, and Gel-DATT under stirring and ultrasonic sound before casting to give the composites as films. Gelatin composite mixture in the process of casting gave stable suspensions, while in the composites based on Gel-DAT and Gel-DATT immediate precipitation occurred. TGA of the dried composite films confirmed the composition of the samples as set during the synthesis. In the Gel-DAT and Gel-DATT composites, the Ca/P ratio ranged between 1.33 and 1.81, which indicated a change in material composition during composite formation, e.g. through exchange of PO_4^{3-} and OH^- ions by HPO_4^{2-} ions (see Table 2). The composites were investigated with wide-angle X-ray spectroscopy (WAXS). X_s increased for both HAp Type 1 and Type 2, however, HAp Type 1 exhbited the higher increase, which was possibly due to particle agglomeration. X_c of HAp Type 1 did not change, while it decreased for Type 2. Determination of the relative content of single- or triple

helices in the composites was not possible due to the much higher intensity of the HAp peaks.

The morphology of the dry composite films was investigated with scanning electron microscopy (representative picture: see Figure 1). Interestingly, HAp Type 1 gave larger agglomerates in the matrix while for HAp Type 2 no such agglomeration was observed.

[HERE FIGURE 1]

3.2 IR spectroscopy of the composites

The chemical compositions of the composite materials were investigated by IR spectroscopy in order to identify characteristic bands for HAp and gelatins used. The IR spectra of Gel-DAT, Gel-DATT, the HAp Type 1 and 2, and their composites are displayed in Figure 2. Bands representative for the matrix included amides I at ~1650 cm^{-1}, amides II at ~1540 cm^{-1}, and amides III at ~1240 cm^{-1}, corresponding to C=O stretch, N-H in plane bend and C-H stretch, and C-N and N-H stretch in plane. Furthermore, carboxyl bands ascribed to amino acids in the gelatin backbone appear between 1300 cm^{-1} and 1450 cm^{-1}. Bands correlated to the hydroxyapatites were observed in the fingerprint region (~630 cm^{-1} for OH ions, and 960 and 1030-1090 cm^{-1} for PO_4^{3-} ions). In Figure 3, the most obvious shifts of IR bands in the composites compared to the free matrices are highlighted. In Gel-DAT composites at 2800 cm^{-1} to 3000 cm^{-1} either strong shifts of up to 15 cm^{-1} or new bands occurred. For Gel-DATT composites, these shifts were similarly observed, yet the shifts of amino- and carboxyl peaks were much more pronounced. The type and amount of HAp influenced the intensity of the chemical shifts, whereby HAp Type1 had a stronger influence than HAp Type 2. Interestingly, in Gel-DAT composites, the most obvious shifts were in the region of 2800 to 3000 cm^{-1}, while for Gel-DATT composites, shifts of band between 1200 and 1700 cm^{-1} were more pronounced. In gelatin composites, no shifts of IR bands compared to the pure matrix were observed.

(HERE FIGURE 2)

(HERE FIGURE 3)

3.3 Water uptake and swelling

The water-uptake H and the degree of swelling Q at 25 and 37 °C of the pure matrices and the different composites are summarized in Table 2. HAp tended to reduce water-uptake and swelling. Further analysis of the data verified the anticipated decrease of water-uptake and swelling when incorporating higher amounts of HAp. Moreover, Gel-DAT composites remained stable at 37 °C, confirming the effect of HAp on the thermal stabilization of Gel-DAT. HAp Type1 incorporation resulted in significantly less water-uptake and swelling than the introduction of HAp Type2 into Gel-DAT. This was especially significant for Gel-DAT composites at 37 °C. Such a behavior could not be monitored for the related composites since Gel-DATT is stable at 37 °C. The obtained data indicated that Gel-DATT composites have roughly the same water uptake and degree of swelling at 25 and 37 °C, respectively. On the contrary, at higher temperature Gel-DAT composites showed much higher water-uptake and swelling. The elevated level of water-uptake of Gel-DAT / HAp Type 2 composites compared to Gel-DAT / HAp Type 1 composites could be due to a higher free volume present in the HAp Type 2 composites, a higher elasticity in these composites, or due to a different attraction to water of the two types of HAp.

HERE TABLE 2

3.4 Mechanical characterization

Tensile tests were performed on samples equilibrated in water, i.e. on composite hydrogels along with non-functionalized gelatin as reference material (Table 3). The Gel-DATT

composites were too brittle to be measured in tensile tests, therefore, in the following only gelatin and Gel-DAT based materials are discussed.

Tensile tests revealed significant alteration of mechanical performance of the composites with the introduction of HAp. Young's modulus (E) and the maximum tensile strength σ_{max} increased with increasing amount of filler in the composites, while no significant changes for the elongation at break (ε_b) were observed. The trend was generally more pronounced for HAp Type 2 than for Type 1, and the changes were different for the two matrices, e.g. the effect of 20 wt.-% filler in Gel-DAT was similar to the effect of 50 wt.-% filler in gelatin.

HERE TABLE 3

For non-functionalized gelatin, HAp created significant mechanical stiffness and strength without inducing brittleness. However, mechanical performance of Gel-DAT in terms of stiffness and strength exceeded that of native gelatin. Although mechanical properties for the two types of HAp composite materials are in a similar range, Gel-DAT containing HAp Type1 reached a mechanical strength of up to 1 MPa when 50 wt% of HAp was incorporated in the composite. As could be expected, the amount of HAp in the composites had a stronger effect on the mechanical properties than the type of HAp.

Rheological measurements were performed in order to investigate the thermal stability of the composites equilibrated in water. Here the elastic modulus (G'), viscous modulus (G") and complex viscosity (η*) in dependence of the temperature were recorded. The temperature at which the elastic and the viscous moduli intersect is defined as Elastic-Viscous-Transition-Temperature T_{Gel}, above which the material starts to behave more like a liquid rather than like a solid material. In order to determine T_{Gel}, the sample was gradually heated as depicted in Figure 4 showing a typical course of G' and G" for gelatin, for Gel-DAT and for Gel-DAT composites with different HAp ratios (transition temperatures: see Table 3).

HERE FIGURE 4

It can be noted that the crossover of G' and G" increased significantly with increasing amounts of HAp. No influence originating from the type of HAp could be observed.

4. Discussion

The precipitation during the mixing of HAp with Gel-DAT or Gel-DATT solutions during the formation of the composite films was likely due to an interaction between the matrix materials and the filler. As no precipitation occurred with pure gelatin, this phenomenon can be associated with the aromatic functionalization of the materials. The changes of the crystal size X_s and overall crystallinity X_c of the HAp in the composites compared to the pre-fabricated particles can be interpreted in that way, that an association to larger particles happened, and that some crystals dissolved. The larger changes of X_s of HAp Type 1 compared to Type 2 is potentially because of the higher SSA of HAp type 1 and the resulting higher reactivity of this species. Specific interactions between matrix and filler are supported by the shifts of the IR bands in the composites compared to the pure matrices. The range of 2800 cm^{-1} to 3000 cm^{-1} is a rather ambiguous region in terms of data interpretation. Only a few studies are reported that focus on the peaks at 2923 cm^{-1} and 2824 cm^{-1}, which correspond to the stretching mode of the vibration of amino acids belonging to the gelatin polypeptide [43]. Gel-DATT composites exhibited a different dominating pattern of shifts. The shifts observed are either related to Ca^{2+} -COO^- chelation ($RCOO^-$) [44], ascribed by the shift of COO^- at ~1340 cm^{-1} or to PO_4^{3-} and NH_3^+ ionic interaction, identified as band shifts of phosphate and amino groups [45]. The shift attributed to asymmetric stretching of COO^- at 1650 cm^{-1} indicates weakening of the C=O bond in the peptide chain, which was caused by the formation of new bonding interactions between Ca^{2+} and C=O bonds. The shift in the phosphate band for Gel-DATT composites indicated polar interaction with NH_3^+ as well as hydrogen bonding and therefore participation in the interfacial interactions. These alterations of the IR pattern could also be observed with Gel-DAT composites, yet at a less pronounced

level of intensity. These data indicate that the incorporation of HAp resulted in additional physical crosslinks into the networks. In FTIR, bands corresponding to aromatic rings or phenolic OH groups were not observed, therefore this method did not help in directly identifying interactions between surface HAp ions and the aromatic rings or phenolic OH groups of functionalized gelatins. However, the shifts reported above were stronger for matrices with increased aromatic content. This can on the one hand be because of direct interactions between the incorporated phenols and the filler, or because the reaction of DAT and DATT with free amino groups reduced the electrostatic interaction between free carboxylic and amino groups on the gelatin, so that more carboxylates can engage in binding to Ca^{2+}.

Incorporation of HAp resulted in reduced degree of swelling and water-uptake of the polymer-networks. However, the amount of HAp and therefore presumingly the Ca^{2+} ion concentration was crucial. This suggests that HAp strengthens the polymer-network by inducing higher stiffness to the overall network. Water-uptake into a matrix takes place first by filling the free volume of the material and by tight binding of water molecules to functional groups of the polymer, which does not necessarily result in swelling. Further uptake of water is then an equilibrium process between the elasticity of the polymer-network and osmotic pressure of entering water. The less water that penetrates in this third step into the matrix, the stiffer is the network. Since polymer networks with HAp exhibit considerably less swelling than polymer networks without HAp, the HAp crystals seem to strengthen the system by physical crosslinking of polymer strands through labile Ca^{2+}-ions on the surface. These additional crosslinks not only reduce water-uptake/swelling but even increase thermal stability of swollen systems. This is a further hint of the interfacial crosslinking ability of Ca^{2+} from HAp. Furthermore, samples immersed in water retained their shape and integrity with incorporation of HAp. This is not the case for the Gel-DAT matrix alone. Samples lost integrity at 37 °C within 24h because of a higher mobility polymer-strand when Ca^{2+} crosslinks are missing. Additionally, the water-uptake and swelling tests demonstrated the different influence of HAp Type1 and Type2 in Gel-DAT. This can particularly be inferred

from the data obtained for 50 wt.-% content of HAp, where a significant difference in water uptake and swelling is obvious. The generally lower uptake of water of Gel-DATT composites compared to Gel-DAT composites can be explained by the increase of the hydrophobicity of the matrix.

As suggested by the changes of the IR spectra, the increase in E modulus and σ_{max} of samples with 50 wt.-% HAp incorporated can also be explained by physical interaction between labile ions of HAp and free reactive sites of the Gel-DAT. These free reactive sites are most likely π-electrons provided by the aromatic groups of the functionalized gelatins. The proposed interfacial interaction can be described as a physical crosslinking of different strands of gelatins via Ca^{2+} ions provided by HAp. This interaction is reported in literature and suggests a stabilization of the Gel-DAT system [31,32]. Results of mechanical testing imply that a considerable amount of HAp is necessary to effectively strengthen the system. The additional crosslinking tends to enhance the rigidity and overall-strength of the network which in turn results in a higher E modulus and σ_{max} respectively.

Thermal stability under shear stress is raised up to 85 °C with incorporation of HAp into the system. Gel-DAT without HAp dissolves at around 40 °C. This effect is a strong testimony of effective physical crosslinking of gelatin strands by HAp. Presumingly Ca^{2+} ions of HAp are the key to the increase of thermal stability. Again a minimum concentration of HAp seems necessary to effectively strengthen thermal the resistance of the polymer-network. The reduced mobility of the polymer-strands is to be considered as key feature for thermal stability. This in turn leads to the observed results, which states that stronger networks exhibit better thermal resistance. Altogether, the potential interactions in the composites are summarized in Figure 5.

HERE FIGURE 5

Altogether, the type of filler did not have a major effect on the composite macroscopic properties when comparing composites with equal amount of filler. A possible explanation can be seen in Figure 1, where agglomerates of the HAp Type 1 are visible. If these large agglomerates would consist only of HAp, not such a strong effect on the macroscopic properties of the composites would be expected, contrary to what was observed. More likely is that the agglomerates consisted of HAp particles connected by polymer chains, so that the strong interaction between matrix and filler were simultaneously responsible for the increase in Young's modulus and maximum tensile strength as well as for the agglomeration. The larger size of the agglomerates compared to the putatively homogeneously distributed HAp Type 2 particles is then compensated by the better interaction with the matrix. The reason for the agglomeration of HAp Type 1 might be the higher SSA and lower crystallinitiy of this material.

5. Conclusions

The formation of composites from gelatin functionalized with increasing numbers of tyrosine derived phenolic groups with hydroxyapatites gave materials with much reduced degree of swelling. Shifts of IR bands indicated direct interactions between matrix and filler, however, as these interactions were dependent on the type of matrix the aromatic groups introduced in Gel-DAT and Gel-DATT seem to have directly contributed to the interaction. Young's moduli and maximum tensile strengths of the composites increased with the amount of HAp but were not dependent on the type of HAp. The increasing mechanical strength was not accompanied by increased brittleness of the materials. Even at equilibrium swelling the hydrogel composites reached Young's moduli up to 2 MPa, which is much higher than typically observed in hydrogels and is close to cancellous bone (3.5 MPa). Furthermore, the thermal stability of the network was increased to above 85 °C. These observations can be explained by additional physical crosslinking of the networks by interactions between the matrix and Ca^{2+} ions of the filler. Interestingly, these types of interactions have been

observed for biomineralized composites but not for composites formed by mixing HAp particles and dissolved polymer matrices.

The pure matrices have shown Young's moduli in the dry state in the low GPa range [36]. In a potential application as bone fillers or coatings of implants, this should result in good protection against abrasion. This should be all the more true for the composites, since a similar increase in mechanical properties was observed in the equilibrium swollen state. Theoretically, after being implanted in the dry state, the low swelling of the investigated materials would then result in an adjustment of the materials to the mechanical properties needed in the biological environment without disintegrating immediately. These composites would therefore be an interesting field of study as bone fillers and implant coatings.

Acknowledgements

We thank Ben Pierce and Karolin Schmälzlin for help in the preparation of the manuscript.

Role of the funding source

This work was partially funded by the Deutsche Forschungsgemeinschaft (DFG) through SFB subproject B5 – thank you. The funding agency did not participate in study design, the collection, analysis, or interpretation of data, the writing of the report, or in the decision to submit the paper for publication.

References:

[1] Madbouly S, Lendlein A, Shape-Memory Polymer Composites. Adv Polym Sci 2010;226:41–95.
[2] Fu SY, Feng XQ, Lauke B, Mai YW, Effects of particle size, particle/matrix interface adhesion and particle loading on mechanical properties of particulate–polymer composites. Composites B. 2008;39:933–961.
[3] Alexandre M, Dubois P. Polymer-layered silicate nanocomposites: preparation, properties and uses of a new class of materials. Mater Sci Eng R 2000;28:1–63.
[4] Lau KT, Gu C, Hui D. A critical review on nanotube and nanotube/ nanoclay related polymer composite materials. Composites Part B 2006;37:425–36.
[5] Padilla S, . Izquierdo-Barba I. Vallet-Regí M, High Specific Surface Area in Nanometric Carbonated Hydroxyapatite, Chem Mater. 2008;20:5942-5944.
[6] Kilian O, Wenisch S, Karnati S, Baumgart-Vogt E, Hild A, Fuhrmann R, Jonuleit T, Dingeldein E, Schnettler R, Franke RP, Observations on the microvasculature of bone

defects filled with biodegradable nanoparticulate hydroxyapatite. Biomaterials 2008;29:3429–3437.
[7] Thein-Han WW, Shah J, Misra RDK, Superior in vitro biological response and mechanical properties
of an implantable nanostructured biomaterial: Nanohydroxyapatite–silicone rubber composite. Acta Biomater 2009;5:2668–2679.
[8] Thein-Han WW, Misra RDK Biomimetic chitosan–nanohydroxyapatite composite scaffolds for bone tissue engineering. Acta Biomater 2009;5:1182–1197.
[9] Yu H, Wooley PH, Yang SY, Biocompatibility of Poly-ε-caprolactone-hydroxyapatite composite
on mouse bone marrow-derived osteoblasts and endothelial cells. J Orthop Surg Res 2009;4:5.
[10] Barbieri D, Renard AJS, de Bruijn JD, Yuan H, Heterotropic Bone Formation by Nano-Apatite Containing Poly(D,L-Lactide) Composites. EurCells Mater 2010;1 9: 252-261.
[11] Yu HS, Hong SJ, Park JH, Jeong I, Kim HW, Bioactive and Degradable Composite Microparticulates for
the Tissue Cell Population and Osteogenic Development. Adv Eng Mater 2009;11:B162-B168.
[12] Cimerman M, Cör A, Ceh M,. Kristan A, Pizem J, Tonin M, Microstructural analysis of implant-bone
interface of hydroxyapatite-coated and uncoated Schanz screws. J Mater Sci Mater Med 2005;16:627– 634.
[13] Davies JE, Bone bonding at natural and biomaterial surfaces. Biomaterials 2007;28:5058–5067.
[14] Cazalbou S, Eichert D, Rey C, Adaptative physico-chemistry of bio-related calcium phosphates, Chem Mater. 2004;16:2148-2153.
[15] Marra KG, Szem JW, Kumta PN, DiMilla PA, Weiss LE, In vitro analysis of biodegradable polymer blend/ hydroxyapatite composites for bone tissue engineering. J Biomed Mater Res 1999;47:324–335.
[16] Yang W, Yin G, Zhou D, Gu J, Li Y, In Vitro Characteristics of Surface-Modified Biphasic Calcium Phosphate/Poly(L-Lactide) Biocomposite. Adv Eng Mater 2010;12:B128-B132.
[17] Hayakawa T, Mochizuki C, Hara H, Fukushima T, Yang F, Shen H, Wang S, Sato M, Influence of Apatite Crystallinity in Porous PLGA/Apatite Composite Scaffold on Cortical Bone Response. J Hard Tissue Biol 2009;18:7-12.
[18] Chuenjitkuntaworn B, Inrung W, Damrongsri D, Mekaapiruk K, Supaphol P, Pavasant P, Polycaprolactone/ Hydroxyapatite composite scaffolds: Preparation, characterization, and in vitro and in vivo biological responses of human primary bone cells. J Biomed Mater Res A 2010;94A:241-251.
[19] Nakamura Y, Yamaguchi M, Okubo M, Matsumoto T. Effects of particle size on mechanical and impact properties of epoxy resin filled with spherical silica. J Appl Polym Sci 1992;45:1281–9.
[20] Zhang Q, Tian M, Wu Y, Lin G, Zhang L. Effect of particle size on the properties of Mg(OH)2-filled rubber composites. J Appl Polym Sci 2004;94:2341–6.
[21] Wu CL, Zhang MQ, Rong MZ, Friedrich K. Silica nanoparticles filled polypropylene: effects of particle surface treatment, matrix ductility and particle species on mechanical performance of the composites. Compos Sci Technol 2005;65:635–45.
[22] Thio YS, Argon AS, Cohen RE. Role of interfacial adhesion strength on toughening polypropylene with rigid particles. Polymer 2004;45:3139–47.
[23] Zahn D, Hochrein O, Kawska A, Brickmann J, Kniep R, Towards an atomistic understanding of apatite–collagen biomaterials: linking molecular simulation studies of complex-, crystal- and composite-formation to experimental findings. J Mater Sci 2007;42:8966–8973.
[24] Simon P, Schwarz U, Kniep R, Hierarchical architecture and real structure in a biomimetic nano-composite of
fluorapatite with gelatine: a model system for steps in dentino- and osteogenesis? J Mater Chem 2005;15:4992–4996.

[25] Rizzi SC, Ehrbar M, Halstenberg S, Raeber GP, Schmoekel HG, Hagenmüller H, Müller R, Weber FE, Hubbell JA, Recombinant Protein-co-PEG Networks as Cell-Adhesive and Proteolytically Degradable Hydrogel Matrixes. Part II: Biofunctional Characteristics Biomacromolecules. 2006;7:3019-3029
[26] Shastri VP, Lendlein A Materials in Regenerative Medicine. Adv Mater. 2009;21:3231-3234.
[27] Olsen D, Yang C, Bodo M, Chang R, Leigh S, Baez J, Carmichael D, Perälä M, Hämäläinen ER, Jarvinen M, Polarek J, Recombinant collagen and gelatin for drug delivery. Adv Drug Deliv Rev. 2003;55:1547-67.
[28] Lendlein A, Neuenschwander P, Suter UW, Tissue-compatible multiblock copolymers for medical applications, controllable in degradation rate and mechanical properties. Macromol Chem Phys. 1998;199; 2785-2796.
[29] Lendlein A, Colussi M, Neuenschwander P, Suter UW, Hydrolytic degradation of phase-segregated multiblock copoly(ester urethane)s containing weak links. Macromol Chem Phys. 2001;202:2702-2711.
[30] Lendlein A, Zotzmann J, Feng YK, , Alteheld A, Kelch S, Controlling the Switching Temperature of Biodegradable, Amorphous, Shape-Memory Poly(rac-lactide)urethane Networks by Incorporation of Different Comonomers. Biomacromolecules. 2009;10:975-982.
[31] Kanungo BP, Gibson LJ, Density–property relationships in collagen–glycosaminoglycan scaffolds. Acta Biomater. 2010;6:344–353.
[32] Engler AJ, Sen S, Sweeney HL, Discher DE, Matrix Elasticity Directs Stem Cell Lineage Specification. Cell. 2006;126:677–689.
[33] Reddy AS, Sastry GN, Cation [M) H+, Li+, Na+, K+, Ca2+, Mg2+, NH4+, and NMe4+] Interactions with the
Aromatic Motifs of Naturally Occurring Amino Acids: A Theoretical Study. J Phys Chem A. 2005;109:8893-8903.
[34] Montero A, Mann E, Chana A, Herradon B, Peptide-Biphenyl Hybrids as Calpain Inhibitors. Chem Biodiv. 2004;1:442-457.
[35] S. R. Fahnestock, A. Steinbuchel, Biopolymers, Vol. 8 (Polyamides and Complex Proteinaceous Materials II), Wiley-VCH, Weinheim, 2003, Chapter 6.
[36] Tronci G, Neffe AT, Pierce BF, Lendlein A, An Entropy-Elastic Gelatin-Based Hydrogel System. J Mater Chem. 2010, Advance article DOI 10.1029/c0jm00883d.
[37] Zaupa A, Neffe AT, Pierce BF, Lendlein D Hofmann D, A molecular dynamic analysis of gelatin as an amorphous material: Prediction of mechanical properties of gelatin systems. IJAO, cond. accepted.
[38] Neffe AT, Zaupa A, Pierce BF, Hofmann D, Lendlein A, Knowledge-Based Tailoring of Gelatin-Based
Materials by Functionalization with Tyrosine-Derived Groups. Macromol. Rapid Commun. 2010;31:1534-1539.
[39] Zaupa A, Neffe AT, Pierce BF, Noechel U, Lendlein A, The influence of gelatin functionalization with tyrosine-derived moieties on the formation of helices. Biomacromolecules, submitted.
[40] Young AM, Hoa SM, Abou Neel EA, Ahmed I, Barralet JE, Knowles JC, Nazhat SN, Chemical characterization of a degradable polymeric bone adhesive containing hydrolysable fillers and interpretation
of anomalous mechanical properties. Acta Biomater. 2009;5:2072–2083.
[41] Peroglio M, Gremillard L, Eglin D, Lezuo P, Alini M, Chevalier J, Evaluation of a new press-fit in situ setting composite porous scaffold for cancellous bone repair: Towards a ‘‘surgeon-friendly” bone filler? Acta Biomater. 2010;6:3808–3812.
[42] Pierce BF, Tronci G, Rößle M, Neffe AT, Lendlein A, Photocrosslinkable conetworks from glycidylmethacrylated gelatin and poly(ethyleneglycol) methacrylates as bone fillers. Clin Orthoped Rel Res. submitted.
[43] Sivakumar M, Rao KP, Preparation, characterization and in vitro release of gentamicin from coralline hydroxyapatite–gelatin composite microspheres, Biomaterials 2002;23:3175-3181.

[44] Tampieri A, Celotti G, Landi E, Sandri M, Roveri N, Falini G, Biologically inspired synthesis of bone-like composite: Self-assembled collagen fibers/hydroxyapatite nanocrystals. J. Biomed Mater Res A. 2002;67:618-25.
[45] Teng S, Shi J, Peng B, Chen L, The effect of alginate addition on the structure and morphology of hydroxyapatite/gelatin nanocomposites, Comp Sci Tech. 2006;66:1532-1538.

Legends and Tables:

Table 1: Summary of the obtained properties of Carbonated HA powders. AR: aspect ratio, X_s: Crystal size, X_c Degree of crystallinity, SSA: Specific Surface Area, Ca/P: Calcium/Phosphor ratio.

	AR	X_s [nm]	X_c [%]	SSA [m^2/g]	Ca/P	CO_3^{2-} [wt%]
HA Type1	~2.5	~16	<5	162	1.77	2
HA Type2	~2.5	~31	48	52	1.62	1.1

Figure 1: Cross-sections of Gel-DAT-composites with different amounts of HA Type1 (a-50wt%; b-20wt%) and HA Type2 (c-50wt%; d-20wt%).

Figure 2: IR spectra of matrices, HAp, and composites. Top left) DAT/HAp Type 1, top right) DAT/HAp Type 2, bottom left) DATT/HAp Type 1, bottom right) DAT/HAp Type 2. — matrix (pure), --- HAp (pure), — 20 wt.-% HAp, --- 50 wt.-% HAp.

Figure 3: Shifts of bands in the IR spectra of the composites compared to the free matrices. a) DAT/HAp Type 1, b) DAT/HAp Type 2, c) DATT/HAp Rype 1, d) DAT/HAp Type 2. — matrix (pure), --- HAp (pure), — 20 wt.-% HAp, --- 50 wt.-% HAp.

Table 2: Water Uptake and swelling of the matrices and composites. Diss: Sample dissolved under these conditions.

Material		Ca/P ratio	X_x	X_c	H (25 °C)	Q (25 °C)	H (37 °C)	Q (37 °C)
Matrix	Filler		[nm]	[%]	[wt.-%]	[Vol.-%]	[wt.-%]	[Vol.-%]
G0	-				2340±380	2740±500	Diss.	Diss.
GEL-DAT	-				400±45	600±60*	Diss.	Diss.
GEL-DATT	-				425±45	600±60	435±85	615±100
GEL-DAT	20 wt.-% Type 1	1.33	28	<5	290±15	515±50	785±65	1230±90
GEL-DAT	50 wt.-% Type 1	1.38	28	<5	180±10	410±20	410±70	800±115
GEL-DAT	20 wt.-% Type 2	1.41	42	26	285±35	555±50	1070±240	1815±380
GEL-DAT	50 wt.-% Type 2	1.44	42	37	200±40	475±75	650±85	1300±155
GEL-DATT	20 wt.-% Type 1	1.36	28	<5	145±10	300±15	180±30	350±45
GEL-DATT	50 wt.-% Type 1	1.50	28	<5	130±25	270±20	120±30	265±40
GEL-DATT	20 wt.-% Type 2	1.44	35	30	140±5	290±10	300±30	505±45
GEL-DATT	50 wt.-% Type 2	1.81	42	60	100±5	240±10	110±25	255±35

Table 3: Values obtained from mechanical testing together with calculated standard deviation. [a]: From tensile tests. [b]: from rheological measurements. Here no standard deviation is given, since only three replicas were measured of each sample and the minimal number for statistic analysis is generally regarded as being five.

Matrix	gelatin		Gel-DAT				
Filler	0	50wt% Type2	0	20wt% Type1	20wt% Type2	50wt% Type1	50wt% Type2
E [kPa][a]	215±60	570±180	340±55	620±85	415±60	1760±260	1860±280
σ_{max} [kPa][a]	70±30	230±40	100±20	100±50	210±70	1070±170	430±140
ε_b [%][a]	16±4	21±6	20±9	15±3	22±9	27±3	17±5
T_{Gel} [°C][b]	37	38-42	37	42-45	42-47	>85	>85

Figure 4: Representative course of temperature dependant G' (black line), G" (black dotted line), and η (grey line) for pure gelatin (a) and Gel-DAT (b) and Gel-DAT composites containing 20 wt% HAp (c) and 50 wt.-% HAp Type 1 (d). T_{gel} is labeled with the vertical dashed line.

Figure 5: Overview of the potential interactions stabilizing the composites. Association of protein chains into collagen-like triple helices is the reason for gelation of unmodified gelatin gels below T_{Gel}. Aromatic substituents have been shown on the one hand to decrease the triple helix formation but on the other hand to generate new crosslinks by □□-interactions. In the composites, chelation of Ca^{2+} ions on the surface of the HAp fillers, and interactions between the aromatic rings and the Ca^{2+} ions form additional physical netpoints contributing to the mechanical properties of the composites.

Figure 1 a/b

Click here to download high resolution image

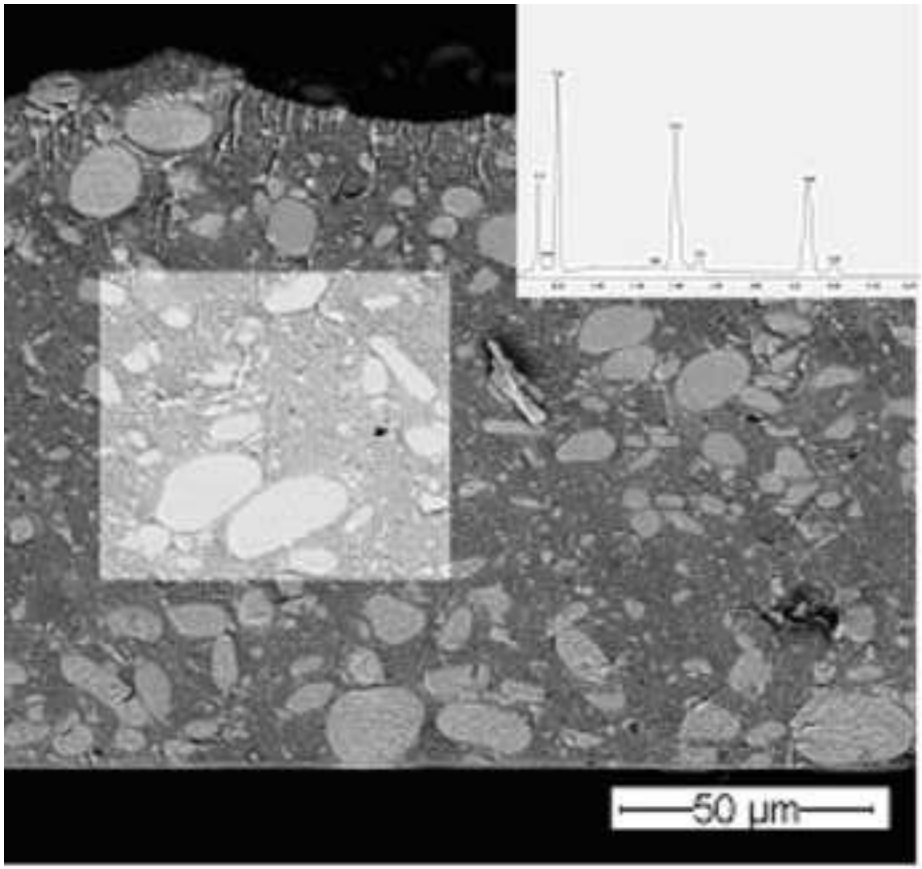

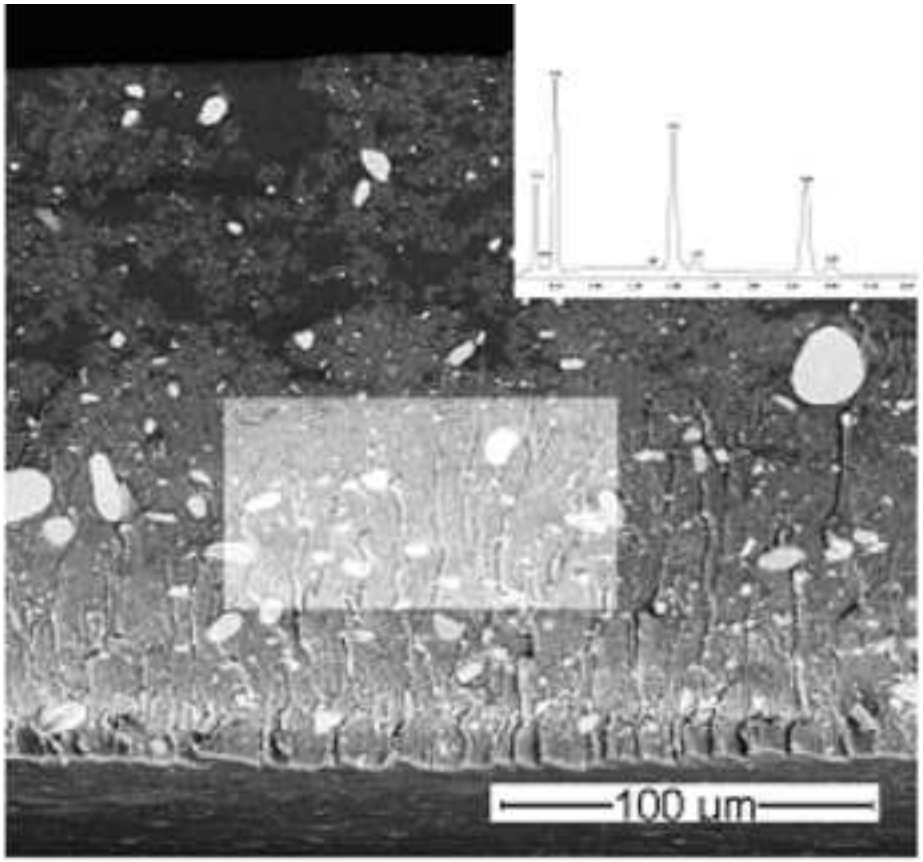

Figure 1 c/d

Click here to download high resolution image

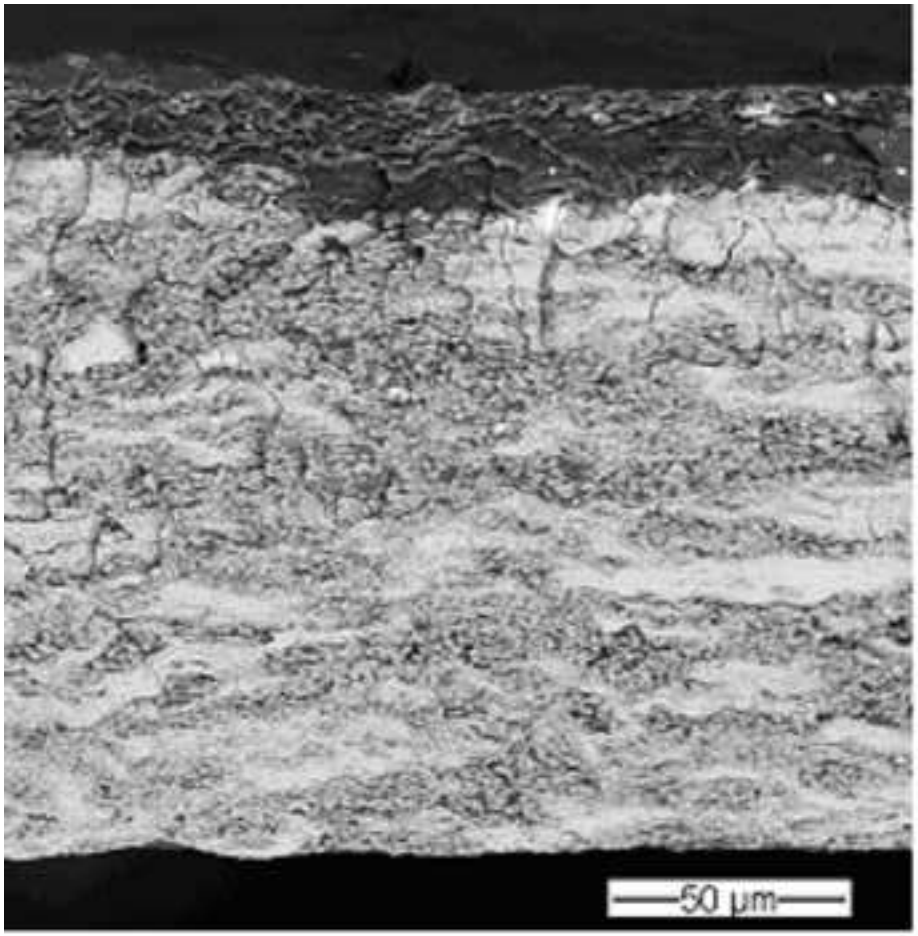

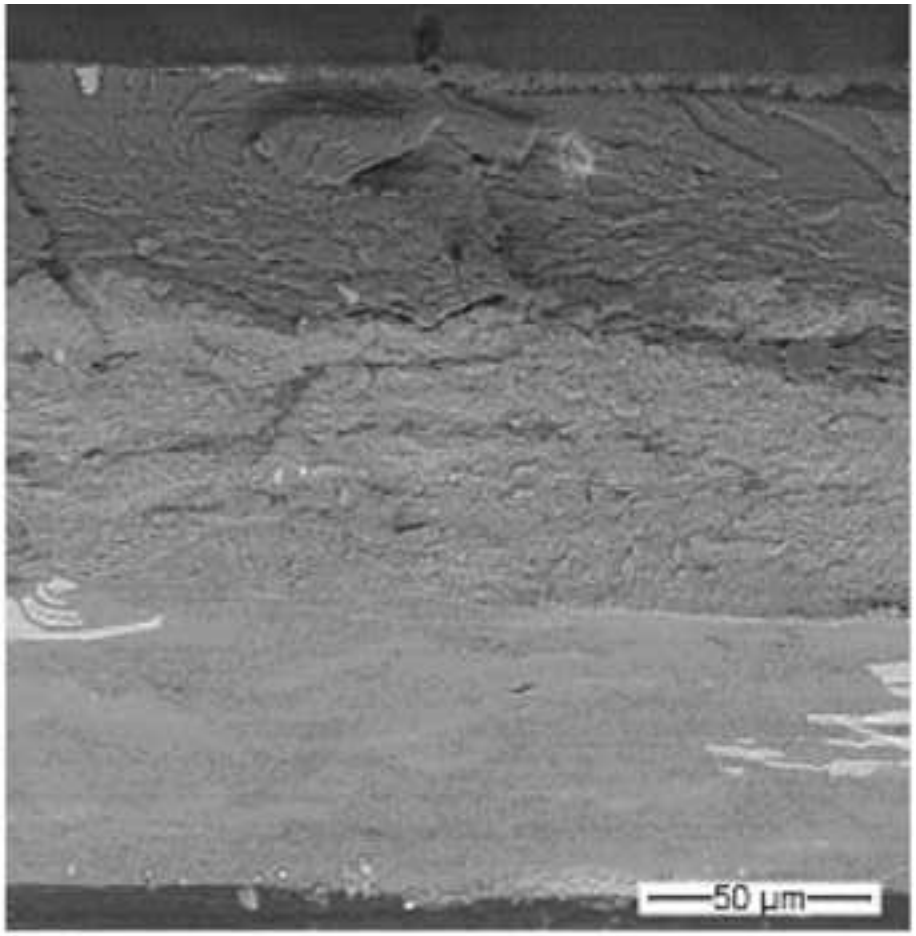

Figure 2

Click here to download high resolution image

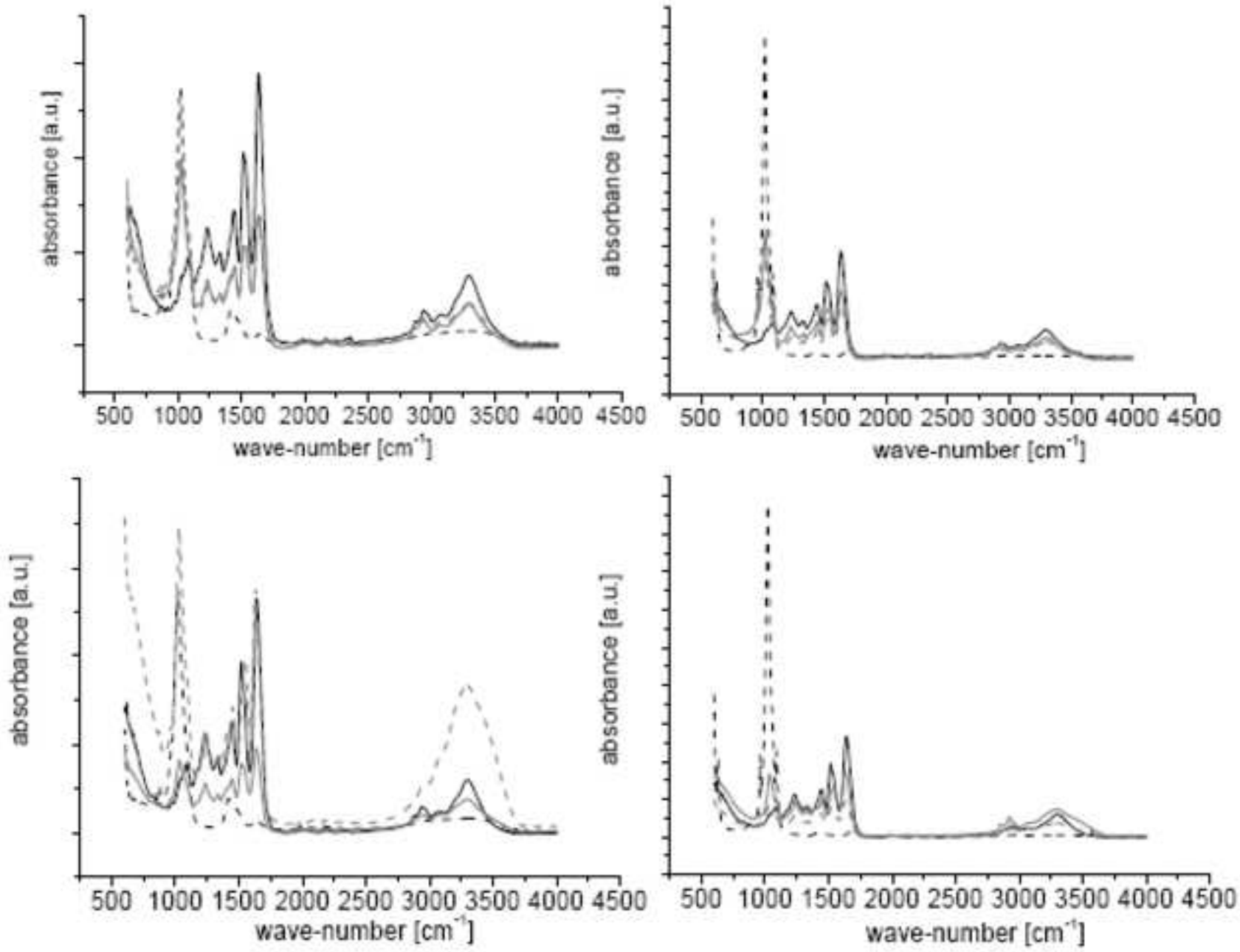

Figure 3

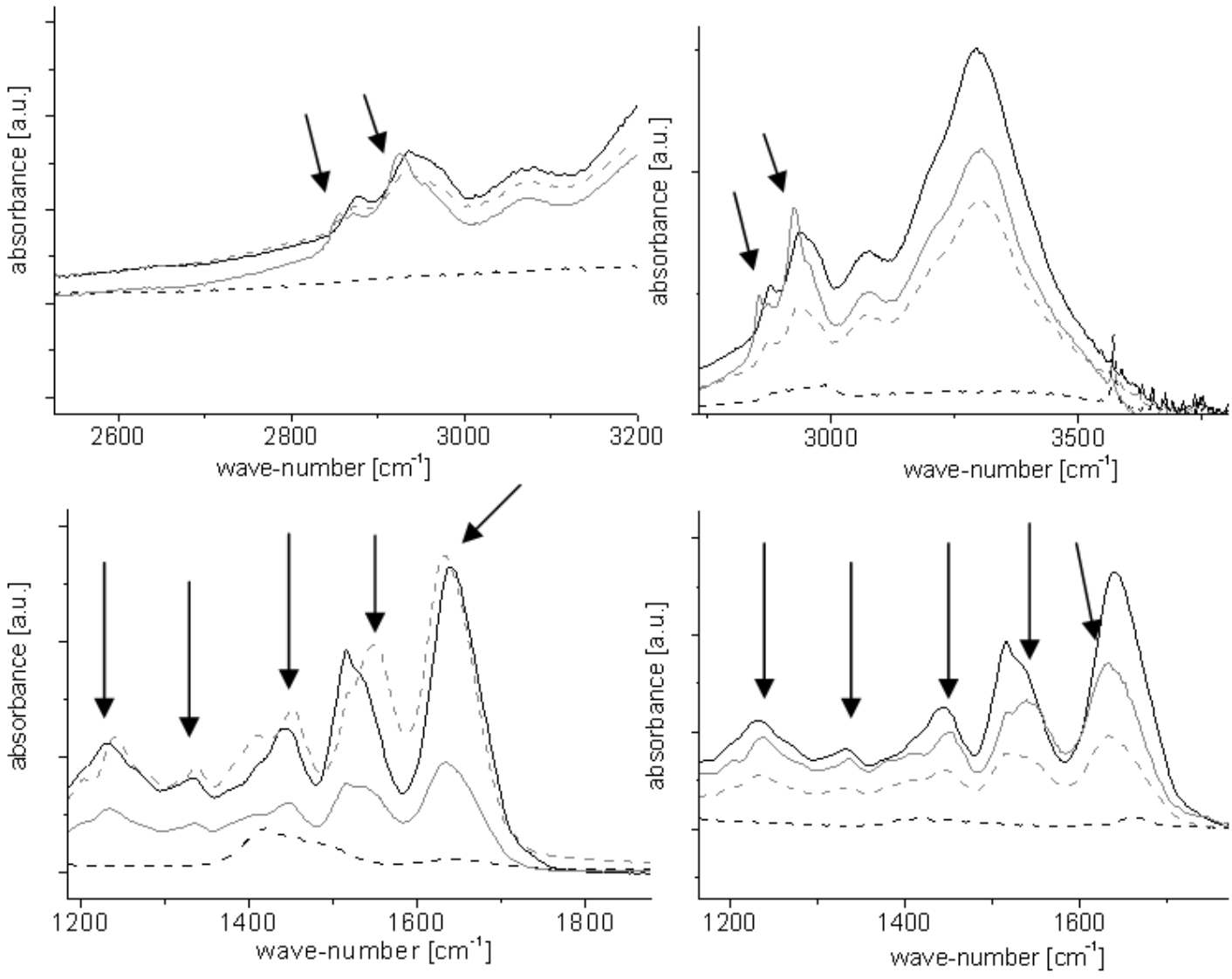
absorbance [a.u.]
2600
2800
3000
3200
wave-number [cm-1]
absorbance [a.u.]
3000
3500
wave-number [cm-1]
absorbance [a.u.]
1200
1400
1600
1800
wave-number [cm-1]
absorbance [a.u.]
1200
1400
1600
wave-number [cm-1]

Figure 4

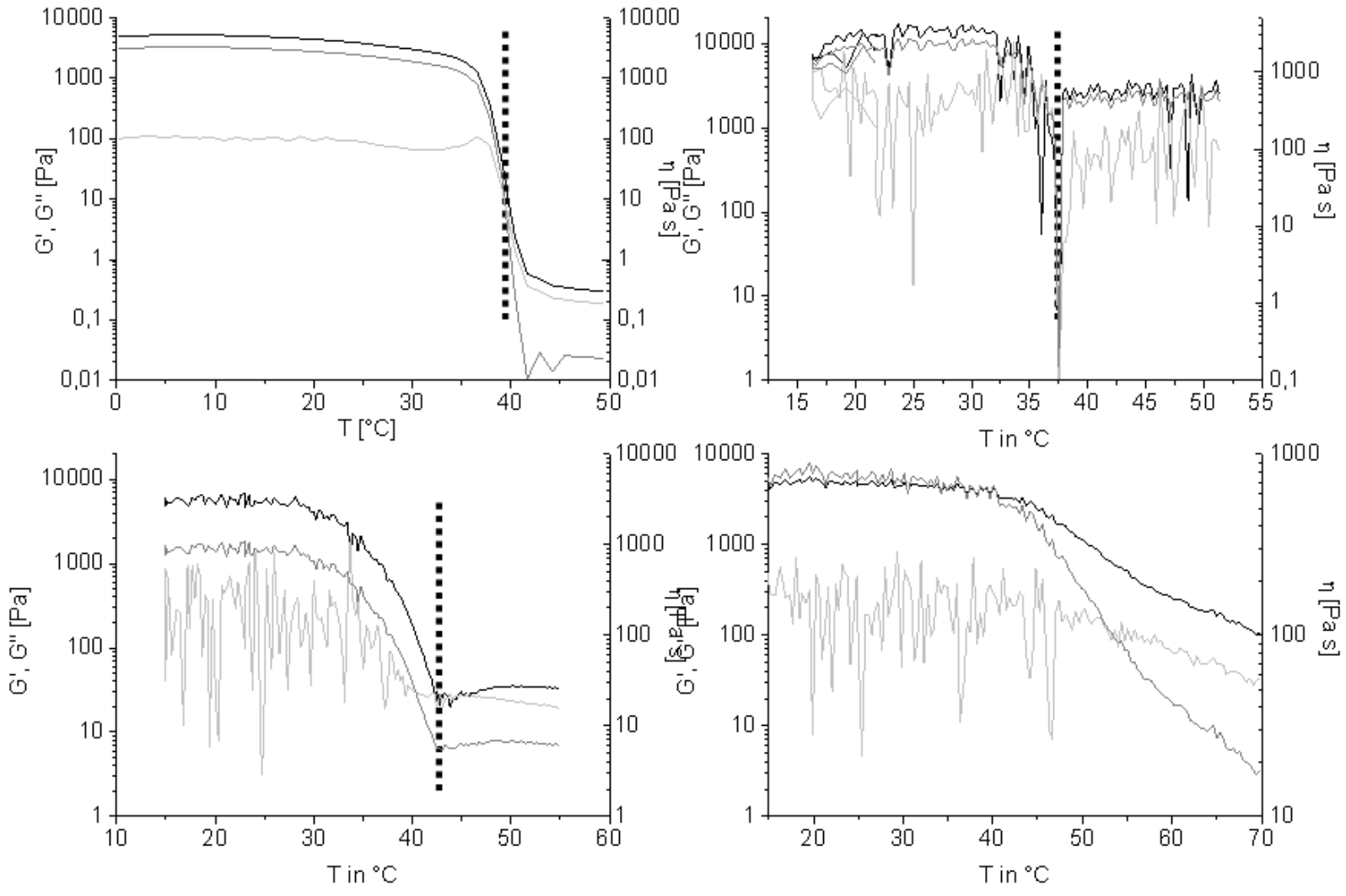

Figure 5